UNCERTAINTY QUANTIFICATION IN SPACE OBJECT REENTRY PROBLEMS

F. Sanson[(1)], JM. Bouilly[(2)], and PM. Congedo[(3)]

[(1)]200 Avenue de la Vieille Tour, 33405 Talence, France,Email:francois.sanson@inria.fr
[(2)]Airbus Safran Launchers,Rue du General Niox, 33165 Saint-Medard-en-Jalles,France,
Email:jean-marc.bouilly@airbusafran-launchers.com
[(3)]200 Avenue de la Vieille Tour, 33405 Talence, France,Email:pietro.congedo@inria.fr

ABSTRACT

The accurate prediction of a reentering space object and its impact zone is a complex problem by the diversity of the physics involved. Numerical models simulating reentry events have to make simplifying assumptions in order to get an impact zone estimate. Along this line, some physical parameters or scenarii such as the fragmentation sequence or the atmosphere state, are chosen arbitrarily. In this work,the uncertainty due to simplifying assumptions in the atmosphere modelling and the lack of knowledge in the characteristics of the material at use are investigated in order to assess the reliability of the prediction. Uncertainty Quantification methods have been applied to reentry problems but only including a limited amount of uncertain parameters due to the computational cost of classical uncertainty quantification methods in high dimension. In this work a large number of uncertain variables are included (50) in order to account for the atmosphere uncertainty and our lack of understanding of the material behaviours during a reentry. Due to the extremely high dimensionality of the problem a Monte Carlo estimation of the uncertainties is carried out. Four simple cases involving a sphere reentering the atmosphere are investigated using a solver developed by Airbus Safran Launchers (ASL). Finally, a method for estimating reliable impact zone at very low level of probability of failure are presented and assessed in one of the four cases

Key words: uncertainty quantification,space object reentry,multi physics problems .

1. INTRODUCTION

Large space object are regularly observed reentering the Earth atmosphere. Most of them are man made object usually referred as space debris as they are solely inertial object, uncontrollable and of no use for human operations. For those massive objects, accurate estimation of the potential impact zone on the ground and subsequently the risk for populations remains an open research problem. In this context, the French Space Operation Act applicable by 2020 to the future Ariane 6 rockets follows two major objectives: a reduction of the debris released at launches and an estimation of the risks associated to every launch. Following this dual objective, ASL is designing reentry plan for each rocket part that is not the payload (boosters, EPC,upper stage, ...) in order to free critical but saturated orbits from new inertial and possibly hazardous rocket parts. Moreover, in order to ensure an optimal protection of human life and activities a global risk estimation has to be estimated prior to the launch. This estimation of the risk includes the risk related to the launch itself (ascending part) but also the reentry of the rocket parts. To this end ASL, is developing a software for predicting the risks associated to re entering parts of Ariane rocket. Due to the complexity of the physics involved during reentry, the scarcity of experiments and the unpredictability of events such as fragmentation, any model trying to predict a reentry suffer from necessary simplifying assumptions and absence of data. In order to assess the reliability of the predictions, uncertainties involved in space object reentries are quantified in this work. In particular, a reliable impact zone containing all the possible impacts for a given scenario with a very high probability has to be estimated. Several space object reentry software have already been developed. The CNES developed an object oriented reentry tool [OS12] and a risk estimation tool [LAA$^+$10]. A Higher fidelity spacecraft oriented break tool have also been developed by ESA [KFLK05] whereas NASA developed its own spacecraft oriented tool [DOSB$^+$05]. Several studies have already shown the potential of UQ techniques to applied space object reentries in order to strenghen the prediction reliability. In [TKV$^+$15], the authors compare four different uncertainty propagation methods: the Polynomial Chaos Expansion (PCE) approach [LMK10], an ANOVA decomposition based approach referred as Uncertainty Quantification-High Dimensional Model Representation (UQ-HDMR), a Generalized Kriging model and a polynomial metamodel based on Tchebycheff polynomials on sparse grids in the case of orbit propagation. They show the UQ-HDMR tends to perform better than the other methods. The particular case of reentry of reusable objects have been explored in [BHW11], [HB12] . In particular, PCE is used to prop-

Proc. 7th European Conference on Space Debris, Darmstadt, Germany, 18–21 April 2017, published by the ESA Space Debris Office
Ed. T. Flohrer & F. Schmitz, (http://spacedebris2017.sdo.esoc.esa.int, June 2017)

agate aleatory uncertainties whereas epistemic uncertainties are propagated via sampling methods. This method however becomes less and less efficient as the number of uncertainties increases. In [FL05], the authors carried out a UQ analysis with the ESA reentry software SCARAB in a few specific case taking into account the prevailing uncertainties. Similar analysis have been carried out in [RMJ04] using the NASA high fidelity software ORSAT. In this work, the approach is different. As our objective is to include a large number of uncertainties, most of surrogate model approaches presented earlier become highly ineffective as a consequence of the curse of dimensionality. Therefore, in this work no surrogate models are built but the directly the solvers, coupled with a Monte Carlo and Importance Sampling approaches are used to quantify uncertainties. This is feasible base the use of simple models developed by ASL.

The rest of this paper decomposes as follow: first an overview of the numerical solutions brought by Airbus Safran Launchers are presented. In the second section, after identification of the main uncertainties a UQ analysis is applied to estimate the uncertainty in the ground hit, the object survivability and a reliable impact zone.

2. PRESENTATION OF ASL SYSTEM OF SOLVERS

A functional approach was adopted by ASL: the specific aspects of the physics involved in the space object reentry modelling are modelled by a specific solver. Aerodynamic forces are computed by a specific solver whereas ablation phenomena are modelled by another one. The solvers are coupled together into a global system to generate a simulation of the whole scenario. In the rest of this section, the components of the system of solvers is presented more into details. After the initial state for the object of interest has been set (position, velocity, shape and composition ....), the first step is the deorbitation that is the calculation of the trajectory from the initial orbit to the actual atmospheric reentry set to an arbitrary altitude of 120 km. This part is computed with a orbit propagator. Once the object re enters the atmosphere, the aerodynamic forces have to be modelled with an additional solver. The fragmentation solvers (second step) model the efforts applied by the atmosphere to the object. They compute the aerodynamic effort and heat flux and the tank explosion risk. The fragmentation step yields the fragments of the initial object along with their shape, position and velocity. Then, the fragments are propagated down to the surface of the Earth during the third step called survivability and propagation. The code identifies the fragments that will hit the ground (not be completely ablated) and for those fragments hitting the surface, the code computes their energy and impact regions. Finally, for the fourth step the impact regions are compared with human repartition maps to compute the human risk. Each step requires specific set of solvers. As a result the number of inputs quantities and hence the number of uncertain variables is extremely high (order of 100) and therefore the straightforward application of classical UQ method can be challenging. In this work the Monte Carlo approach is chosen in order to bypass the curse of dimensionality. In this work however, only part of the ASL system of solver is used. In particular a trajectory integrator is coupled with an atmosphere model and an ablation solver in order to estimate the impact zone or burn up altitude of a reentering object.

3. METHODOLOGY

In this section the hypotheses used in the uncertainty modelling are presented along with the uncertainty quantification methods used. In particular, the Monte Carlo approach used to quantify the uncertainty and compute the sensitivity indices are quickly reviewed. Finally, the concepts used to derive the low probability quantiles such as importance sampling are presented.

3.1. Presentation of the uncertainties

In this work, two groups of uncertainties have been identified. The first main source of uncertainty chosen in this work is the atmosphere model. The model routinely used at ASL is US62. This simple model holds under restrictive hypotheses [SDW62]. In order to increase the robustness of our predictions, the temperature and the density are modelled as uniform random variables. Since the atmosphere temperature and density depend on the altitude, the temperature and density are perturbed at 21 altitudes independently. The quantities then are interpolated along the trajectory. The range of density variation is set at 40 %. The range of temperature variation is set at 4 K. Note that the atmosphere uncertainty are modelled with 44 variables.
The second source of uncertainties comes from the uncertain material behaviour when the object flies at supersonic speed through layers of atmosphere. In particular, the evaluation of the heat flux requires the material emissivity, conductivity that depend on the degree of oxidation of the material surface for instance. Besides, in order to study the survivability of the object, the melting temperature has to be estimated along with the enthalpy of fusion and the heat capacity. Except for the material emissivity, experimental campaigns have been carried out at Airbus Safran Launchers in order to estimate those material properties. As any experimental campaign, the uncertainties unavoidably corrupt the results. In this work, the experimental results are directly used along with their associated uncertainties. The emissivity has not been measured and actually depends on the history of the material and more specifically the oxidation process that occurs during a reentry. For this reason, the emissivity is modelled as a uniform random variable while the other quantities are modelled as Gaussian random variables. Since the material heat capacity depends on the temperature, the heat capacity is modelled as a vector of a dozen of independent random variable that are then interpolated by

the solver. Table 3.1 summarize the input uncertainties. Note that, depending on the test case the uncertainty input dimensionality ranges between 55 and 60 variables. this high input dimensionality rules out many classical UQ methods and justifies the use of a Monte Carlo based approach.

Table 1. uncertainty distributions

Quantity	Distribution
Free stream temperature	Uniform vector
Free stream density	Uniform vector
emissivity	Uniform
fusion temperature	Gaussian
fusion enthalpy	Gaussian
material density	Gaussian
heat capacity	Gaussian vector

3.2. Monte Carlo approach for uncertainty quantification and sensivity analysis

In this section, the objective is to estimate the output distribution Y of a solver given its uncertain inputs $(X_1, \cdots, X_n)$. The solver is modelled as a function f such as

$$f(X_1, \cdots, X_n) = Y \tag{1}$$

In the Monte Carlo approach, the moments of Y can be estimated as :

$$E[Y^k] = \sum_j f(x_{1,j}, \cdots, x_{n,j}) \tag{2}$$

Where $x_{1,j}, \cdots, X_{n,j}$ are sampled from the input distribution. Furthermore, the probabilities can be estimated as :

$$P(Y \in A) = \sum_j 1_{f(x_{1,j},\cdots,x_{n,j}) \in A} \tag{3}$$

In the next section, the survivability probabilities are estimated in this fashion. Note that the precision of the Monte Carlo estimates depends on the number of samples and are relatively independent on the dimensionality. This is a major advantage in our case since the number of uncertainties is extremely high. The samples generated by Monte Carlo can be used to estimate the probability density function of Y using a kernel density estimate.

Sensitivity analysis aims at identifying major sources of uncertainty and to quantify their influence on the quantity of interest (QOI). In particular the Sobol indices are classically used in global sensitivity analysis (see [SRA$^+$08] for complete reference). They are defined as :

$$S_i = \frac{E[Var(Y|X_i)]}{Var(Y)} \tag{4}$$

Where X_i a specific input and Y the output distribution. The sobol indices quantify the expected diminution in uncertainty if one variable were perfectly known. We use the estimators as described in [Sal02].

3.3. Low probability quantile estimation

In this section, we show how the problem of estimating the ground impact zone can be reduced to a quantile estimation problem. The simplifying assumptions are presented in the next paragraph. In the rest of the section an original method for deriving quantiles at low probability levels is presented. The approach heavily relies on the Importance Sampling (IS) technique which is quickly reviewed before the presentation of the full algorithm.

Mathematical formulation of the problem .

Note that the impact zone at a given probability is not unique. Further more, it depends on the initial parametrization. Several choices of parametrization are available, the most classic ones are the rectangle or ellipsis. Note however that since the later shapes are parametrized by three scalars one needs to enforce another condition in addition to the fixed probability. One can for instance enforce the zone to be as small as possible in order to add an additional constraint. In our case, since the impact point dispersion on the longitude axis is negligible with respect to the latitude axis, the impact zone is estimated only on the longitude axis. The impact zone is therefore represented with a segment centered in c and of amplitude d. The problem is further simplified by arbitrarily taking c as the mean impact point longitude. Mathematically the problem becomes:

$$\inf_{c,d} P(X \in [c - \frac{d}{2}; c + \frac{d}{2}]) \leq p \tag{5}$$

Where X is the object impact point latitude and p a given probability. If one has an efficient method to estimate numerically $P(X \in [c - \frac{d}{2}; c + \frac{d}{2}])$, then any optimization technique can give a solution of 5 . In cases where p is low (in our case we choose 10^{-6}) a Monte Carlo procedure su as presented in the previous section, can be extremely inefficient. For a classical Monte Carlo probability estimator $\hat{p}$ we have:

$$Var(\hat{p}) = \frac{(1-p)p}{N}. \tag{6}$$

Therefore the relative error scales as:

$$\rho = \sqrt{\frac{1-p}{N \times p}} \simeq \sqrt{\frac{1}{N \times p}} \gg 1 \text{ if } p \ll 1 \tag{7}$$

The only way to have a good estimate of p is to have $N \gg \frac{1}{p} = 10^6$. This is in practice unreachable, especially in our case where $P(X \in [c - \frac{d}{2}; c + \frac{d}{2}])$ is estimated several times for different values of d. The main idea to cut down the computational cost is to use importance sampling. Importance sampling allows the recycling of samples and accelerates the calculation of low probabilities. In the following paragraph, important results from importance sampling are presented. A more thorough description of importance sampling can be found in [MP10]. Note however that the level of probability sought in this work are much lower that the one derived in [MP10].

Importance sampling As mentioned previously, in the case of low probabilities, the Monte Carlo method is not efficient. The main idea behind importance sampling is to sample from on auxiliary distribution in order to improve the estimation. Mathematically, we can write:

$$
\begin{aligned}
P(X \in [c-\frac{d}{2};c+\frac{d}{2}]) &= \int 1_{x\in[c-\frac{d}{2};c+\frac{d}{2}]} p_X(x)dx \\
&= \int 1_{x\in[c-\frac{d}{2};c+\frac{d}{2}]} \frac{p_X(x)}{p_Y(x)} p_Y(x)dx
\end{aligned}
\tag{8}
$$

The last integral can be estimated numerically as :

$$
\begin{aligned}
&\int 1_{x\in[c-\frac{d}{2};c+\frac{d}{2}]} \frac{p_X(x)}{p_Y(x)} p_Y(x)dx \\
&\qquad = \sum_i 1_{X_i'\in[c-\frac{d}{2};c+\frac{d}{2}]} \frac{p_X(X_i')}{p_Y(X_i')}
\end{aligned}
\tag{9}
$$

Where X_i' is sampled according to Y, the auxiliary distribution. The choice of auxiliary distribution is crucial as the optimal one leads to an estimator variance that is asymptotically 0. In this work, the auxiliary distribution is chosen as a mixture of Gaussians with most of their density weight by the outer edge of the impact zone.

Probability integral transform While studying low probability probability it is classical to perform a probability integral transform, to reduce the inputs probability distributions as independent Gaussian random variables. The formulae are given here for the record:

$$X_{phys} = F_{X_{phys}}(\phi^{-1}(U)) \tag{10}$$

And conversely:

$$U = \phi(F^{-1}_{X_{phys}}(X_{phys})) \tag{11}$$

Where U is a standard normal random variable and X_{phys} is the uncertain input variable and $F(x)$ its Cumulative Density Function (CDF). Note that $F(x) = P(X < x)$

Presentation of the algorithm The algorithm presented aims at solving Eq. (1). It is a three step algorithm:

1. Initialization A first run of classical MC is necessary get to a rough estimation of the impact zone. In practice the c is given by the median of the sample and a first estimation of d is given by the length of the output distribution support
2. Determination of the auxiliary distribution: the size of the impact zone is roughly estimated through successive importance sampling. The initial auxiliary distribution is chosen as $N(0, \gamma I)$ in normalized probability space with $\gamma = 1.2$. As d changes in the optimization process, the auxiliary has to be changed. An error criterion based on the variance of the estimator is used to determine when a new auxiliary distribution has to be computed. If the current auxiliary does not allow to accurately estimate $P(X \in [c-\frac{d}{2};c+\frac{d}{2}])$ for the current value of d it has to be changed. The subroutine allowing to compute a new auxiliary distribution is detailed in the next paragraph . Once a good auxiliary distribution has been reached ie. a distribution that can precisely estimate $P(X \in [c-\frac{d}{2};c+\frac{d}{2}])$ with $P(X \in [c-\frac{d}{2};c+\frac{d}{2}]) \simeq p$.
3. Finally a precise optimization algorithm such as Newton can be used to get a precise estimate of the impact zone using the same auxiliary distribution. At this point the same auxiliary distribution can be used.

Note that the expensive part of the algorithm is the evaluation of the solver evaluation when a new auxiliary distribution is computed an a sample is generated. Therefore, the computational cost is directly driven by the number of auxiliary distributions and the number of sample that are necessary to obtain convergence. Therefore the choice of the next one is crucial. In practice, we found that three auxiliary distributions were necessary before reaching the desired level of precision for a given probability with a sample size of 100000 samples at each time.

Generation of a new auxiliary distribution The distributions here are estimated in the standard probability space. For a given outdated auxiliary distribution sample (X_i), and a target impact zone parametrized by d.

1. the samples in (X_i) that land outside the impact zone
2. use those sample to fit a Gaussian mixture and use it as the new auxiliary distribution

Note that the number of components in the Gaussian mixture is crucial and should be taken greater than the expected number of important regions in the standard probability space in order not to eliminate regions of the space. The intuition behind this algorithm is that we want to increase the number of impact points that go beyond the impact zone since the probability of being outside the impact zone sought.

4. PRELIMINARY RESULTS

In this section a simple test case is chosen with one specific code developed by Airbus Safran Launchers. To simulate the impact point, a three degree of freedom trajectory solver coupled with a survivability solver is used to predict the reentry of a 0.8 meter diameter sphere whose shell represents 10 % of the total volume, the rest being empty. The sphere is launched at the speed of 6800 m/s at 120 km altitude. Four specific scenarii are considered: two initial slopes (-1 and -5 degrees) and material (Al2219 and TI6AL4V) are used. Additionally, a fifth scenario for a titanium sphere reentering at the slope of -10 degrees is considered for the computation of low probability quantiles. Those test case are seen as controlled reentry events where the initial conditions are design variables and not uncertainties. Depending on the case under study the quantities of interest are the burn up altitude or the ground impact point.

Table 2. uncertainty distributions

Test case id	Material	initial slope [degree]
1	AL2219	-1
2	AL2219	-5
3	TI6AL4V	-1
4	TI6AL4V	-5

4.1. Aluminium case (1 and 2)

In this case, the sphere is made of aluminium and weights 27 kg. The results presented here are obtained with 200000 Monte Carlo samples. In both cases, the object never reaches the ground but completely burns during the flight. In this context the quantity of interest is the altitude at which the object is completely burnt (burn through altitude). The statistics of this quantity are presented in table 4.1 for cases 1 and 2. Unsurprisingly, the burn up altitude obtained with the steepest slope is the lowest. Note however that in this case, the predictions are extremely precise with a variation coefficient of only 0.06 %. This can be explained by the fact that the trajectories are relatively quick (103 seconds for case 1 and 76 seconds for case 2) with a very simple object geometry. The pdf can also be derived from the MC samples using a kernel density estimation. The pdf of the burn up altitude is represented in Fig. 1 for case 1. Very similar results are obtained for case 2 and hence are not shown for brevity. The distribution is rather symmetrical but with heavier tails than a Gaussian random variable.

Table 3. burn up altitudes for cases 1 and 2

Altitude in meters	Case 1	Case 2
Mean	71446.0	68012.83
Standard deviation	42.75	42.58
Variation coefficient	0.06 %	0.06 %
95 % confidence interval	[71326.7;71562.1]	[67894.5;68132.2]

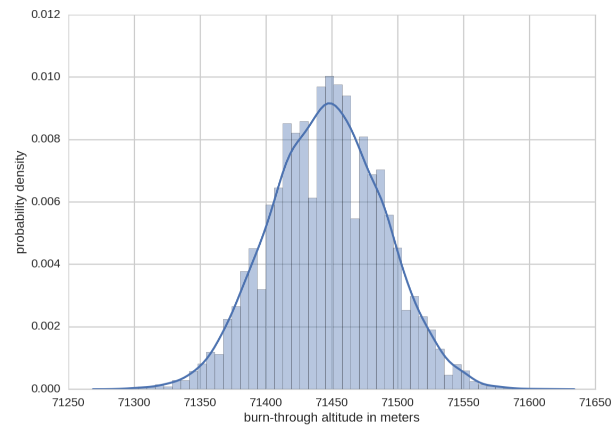

Figure 1. Break-through altitude for case 1

4.2. Identification of the main source of uncertainties

To complete the analysis, a sensitivity analysis is carried out using the Sobol indices (see [SRA+08] for complete reference). In this work, to ease the analysis the atmosphere uncertainty are represented by a single global index. Similarly the heat capacity vector is represented by only one sensitivity index. The sensitivity analysis results are presented in table 4.2. Note that the uncertainty in the burn up altitude comes at 70 % from the material uncertainty whereas the uncertainty in the atmosphere state accounts for 30 % of the uncertainties. Two uncertainty generation mechanisms can be identified. The first one, due to the atmosphere changing state, gradually perturbs the trajectory. Hence, the longer the flight, the more influence the atmosphere variations gain on the QOI uncertainty. On the other hand, the material characteristics directly influence the burn-though time and the aerodynamic of the object as the object changes in shape as it gets ablated. Those changes occur at the end of the trajectory, on a much shorter time scale.

4.3. Titanium case

In these cases, the sphere is made of titanium and weights about 48 kg. Titanium has a greater heat capacity, fusion temperature and fusion enthalpy that make the object more likely to hit the ground. As for cases 1 and 2, the

Table 4. Sobol indices for the burn up altitude

Quantity	Variance contribution
Free stream conditions	32 %
emissivity	7 %
fusion temperature	29 %
fusion enthalpy	2 %
material density	17 %
heat capacity	11 %

results presented in this section are obtained with 200000 samples. Contrary to the previous cases, the object has a significant probability of hitting the ground. For each case one can identify two very distinct scenarii. Either the object burns out completely or it hits the ground, intact or only partially burnt. In Fig. 2, the pdf of the final altitude altitude is plotted. If the altitude is equal to zero, then the object hit the ground, otherwise it is the burn up altitude. Note that in both cases the region where the object burns completely lies above 40 km and that no object burns between 0 and 40km. Moreover the two groups of object also present very different final speeds. The burnt objects disappear at supersonic speeds around 3577 m/s whereas the surviving ones land at much lower speed around 50 m/s. Those virtual objects correspond to the highest heat capacities and enthalpy of fusion. They are able to store and eventually dissipate more heat. Unsurprisingly, the number of objects hitting the ground in the steepest slope case is higher than in the other one. More quantitatively, in case 4, the probability of the object hitting the ground is 0.207 (within 0.3 % error) and in case 3, the probability falls to 0.0625 (within 0.6 % error). In the case where the object hit the ground Fig 3 shows the distribution of the impacts. The distribution of the impact is extremely non symmetric and strongly correlated to the final mass as show in Fig 4. Most of the impacts at a latitude of 7 degrees and correspond to intact objects that have not lost any mass. A much lower amount of objects hit the ground at lower latitude and they correspond to partially ablated, lighter objects. In the next section, a method for estimating reliable impact zone is presented.

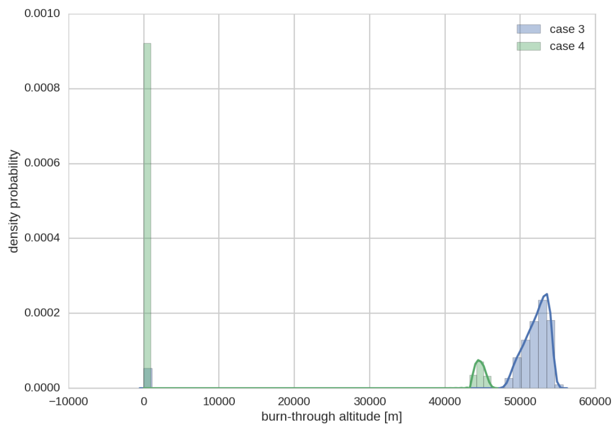

Figure 2. Break-through altitude for case 3 and 4

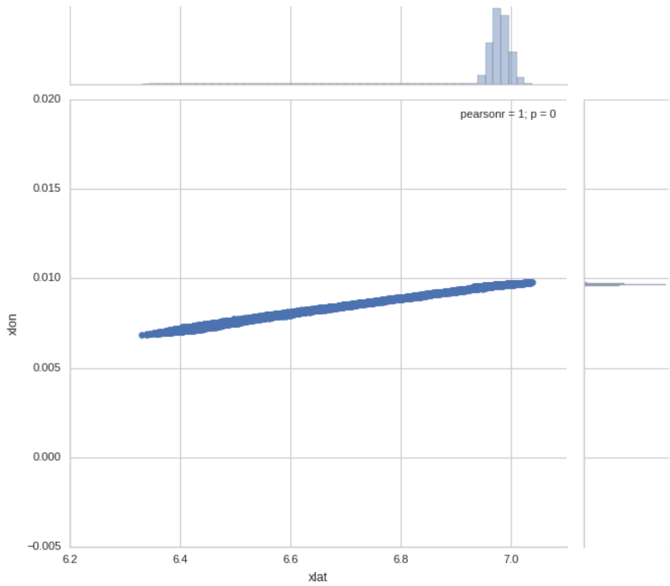

Figure 3. Impact zone

4.4. Impact zone estimation

Estimating a reliable impact zone is a complex task. In the previous section we were able to plot the trace of 200000 possible impacts. This trace however does not provide a reliable impact zone. We call a reliable impact zone for a given probability p a zone where the probability of an impact occurring outside that zone has probability p. In practice p can be extremely small, on the order of 10^{-6}. Estimating low probabilities can be extremely challenging with a straight forward Monte Carlo method, even with a metamodel [MP10] as the number of samples that fall out of the impact zone may be extremely low. In this work we propose an iterative approach using importance sampling in order to estimate a reliable impact zone. In order to demonstrate the potential of the method, a reliable impact zone is computed in the case of a titanium sphere reentering at an angle of -10 degrees. The problem is simplified respect to the modelling of the uncertainties. In particular, the dimensionality of the problem is reduced to seven variables. The atmosphere uncertainties are in this section parametrized by two random variables. Similarly, the heat capacity uncertainties are modelled with only one variable. This is equivalent to considering that the atmosphere uncertainties are independent of the altitude and that the heat capacity uncertainties are independent of the temperature.

In this paragraph we use the algorithm developed in the first section. The target probability is $p = 10^{-6}$. In Fig. 5 the distribution of the impact point longitude

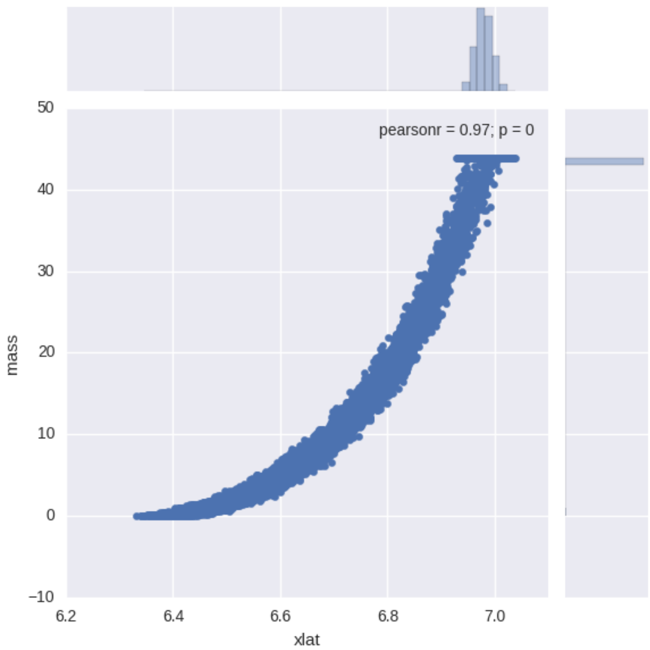

Figure 4. Joint plot final latitude and final mass in kg

is represented with the confidence intervals at 10^{-6}. Note that none of the 200000 samples used to generate the pdf fell outside the zone underlying the limitation of a standard Monte Carlo approach when computing extreme quantiles and reliable impact zones.

Error estimates of the reliable impact zone can be obtained from the Monte Carlo estimation of the probability. Noting v_p, the variance of the estimator $\hat{p}$ of the probability p, then we have that the variance in the radius of the impact zone is:

$$v_r \simeq \frac{v_p}{(\frac{dp}{dr})^2} \tag{12}$$

Thus, in our case with an error of a few percents in the probability estimation, one get a precision of 0.05 % in the radius of the impact interval

4.5. Conclusion

In this work, four space reentry scenarii were presented using simplified ablation solvers coupled with trajectory solvers. For each case, an uncertainty analysis was carried out. In particular, the effect of the atmosphere variations and our lack of understanding of the material behaviour have been investigated. In each case, the burn up altitude along with the impact point distribution is estimated. As expected the aluminium cases never reach the ground but are burnt completely. Conversely, the scenarii using titanium showed more complex behaviours. Two cases could be considered. First the object could be completely ablated and burnt at an altitude above 40km or it

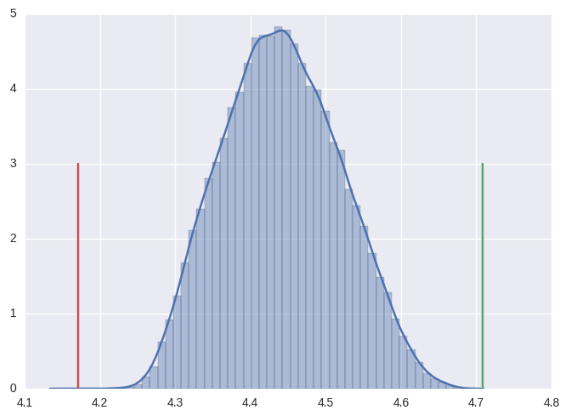

Figure 5. Distribution of the latitude with the reliable impact zone estimation with the impact interval boundary

would reach the ground with a non negligible probability. Note that no object would burn at an altitude below 40km. For the case 1, a sensitivity analysis showed that most of the uncertainty in the burn up altitude stemmed from the uncertain material characteristic. Finally, in a Titanium case, where the ground impact probability is found to be significant, a reliable impact zone is computed with an original algorithm based on importance sampling.

ACKNOWLEDGEMENTS

The authors acknowledge the financial support from Airbus Safran Launchers and the Region Aquitaine for this work. The authors would like to thank Segolene Battandier, Charles Bertorello and Francois Lemaire for the fruitful conversations on space object flight. The authors are also thankful to Celia Finzi, Leila Rhidane and Gregory Pinaud for their input on the material uncertainty characterization.

REFERENCES

BHW11. Benjamin Bettis, Serhat Hosder, and Tyler Winter. Efficient uncertainty quantification in multidisciplinary analysis of a reusable launch vehicle. In *17th AIAA International Space Planes and Hypersonic Systems and Technologies Conference*, page 2393, 2011.

DOSB+05. J Dobarco-Otero, RN Smith, KJ Bledsoe, RM Delaune, WC Rochelle, and NL Johnson. The object reentry survival analysis tool (orsat)-version 6.0 and its application to spacecraft entry. In *Proceedings of the 56th Congress of the International Astronautical Federation, the International Academy of Astronautics, and International Institute of*

Space Law, IAC-05-B6, volume 3, pages 17–21, 2005.

FL05. B Fritsche and S Lemmens. Case studies for uncertainty quantification of a high-fideliety spacecraft oriented break-up tool. In *8th European Symposium on Aerothermodynamics for Space Vehicles Proceedings*, 2005.

HB12. Serhat Hosder and Benjamin Bettis. Uncertainty and sensitivity analysis for reentry flows with inherent and model-form uncertainties. *Journal of Spacecraft and Rockets*, 49(2):193–206, 2012.

KFLK05. G. Koppenwallner, B. Fritsche, T. Lips, and H. Klinkrad. Scarab -a Multi-Disciplinary Code for Destruction Analysis of Space-Craft during Re-Entry. In D. Danesy, editor, *Fifth European Symposium on Aerothermodynamics for Space Vehicles*, volume 563 of *ESA Special Publication*, page 281, February 2005.

LAA+10. B. Lazare, M. H. Arnal, C. Aussilhou, A. Blazquez, and F. Chemama. Electra launch and re-entry safety analysis tool. In *Making Safety Matter*, volume 680 of *ESA Special Publication*, page 46, September 2010.

LMK10. O. P. Le Maître and O. M. Knio. *Spectral methods for uncertainty quantification. With Applications to Computational Fluid Dynamics.* Springer, 2010.

MP10. Jrme Morio and Rudy Pastel. Sampling technique for launcher impact safety zone estimation. *Acta Astronautica*, 66(56):736 – 741, 2010.

OS12. P. Omaly and M. Spel. DEBRISK, a Tool for Re-Entry Risk Analysis. In *A Safer Space for Safer World*, volume 699 of *ESA Special Publication*, page 70, January 2012.

RMJ04. WC Rochelle, JJ Marichalar, and NL Johnson. Analysis of reentry survivability of uars spacecraft. *Advances in Space Research*, 34(5):1049–1054, 2004.

Sal02. Andrea Saltelli. Making best use of model evaluations to compute sensitivity indices. *Computer Physics Communications*, 145(2):280 – 297, 2002.

SDW62. Norman Sissenwine, Maurice Dubin, and Harry Wexler. The us standard atmosphere, 1962. *Journal of Geophysical Research*, 67(9):3627–3630, 1962.

SRA+08. Andrea Saltelli, Marco Ratto, Terry Andres, Francesca Campolongo, Jessica Cariboni, Debora Gatelli, Michaela Saisana, and Stefano Tarantola. *Global sensitivity analysis: the primer*. John Wiley & Sons, 2008.

TKV+15. C Tardioli, M Kubicek, M Vasile, E Minisci, and A Ricciardi. Noise Quantification in Optical Observations of Resident Space Objects for Probability of Detection and Likelihood. In *Proc. AIAA/AAS Astrodynamic Specialist Conference*, Vail, Colorado, 2015.